# 12A.3 High-Resolution Mesoscale Model Setup for the Eastern Range and Wallops Flight Facility

Leela R. Watson*
ENSCO, Inc/Applied Meteorology Unit

Bradley T. Zavodsky
NASA Short-term Prediction Research and Transition Center

## 1. INTRODUCTION

Mesoscale weather conditions can have an adverse effect on space launch, landing, and ground processing at the Eastern Range (ER) in Florida and Wallops Flight Facility (WFF) in Virginia. During summer, land-sea interactions across Kennedy Space Center (KSC) and Cape Canaveral Air Force Station (CCAFS) lead to sea breeze front formation, which can spawn deep convection that can hinder operations and endanger personnel and resources. Many other weak locally driven low-level boundaries and their interactions with the sea breeze front and each other can also initiate deep convection in the KSC/CCAFS area. These subtle weak boundary interactions often make forecasting of operationally important weather very difficult at KSC/CCAFS during the convective season (May-Oct). These convective processes often build quickly, last a short time (60 minutes or less), and occur over small distances, all of which also poses a significant challenge to the local forecasters who are responsible for issuing weather advisories, watches, and warnings. Surface winds during the transition seasons of spring and fall pose the most difficulties for the forecasters at WFF. They also encounter problems forecasting convective activity and temperature during those seasons. Therefore, accurate mesoscale model forecasts are needed to aid in their decision making.

Both the ER and WFF benefit greatly from high-resolution mesoscale model output to better forecast a variety of unique weather phenomena. Global and national scale models cannot properly resolve important local-scale weather features at each location due to their horizontal resolutions being much too coarse. Therefore, a properly tuned model at a high resolution is needed to provide improved capability. This task is part of a multi-year effort in which the Applied Meteorology Unit (AMU) is tuning the Weather Research and Forecasting (WRF) model individually for each range. The goal of the first year was to tune the WRF model based on the best model resolution and run time while using reasonable computing capabilities. [*]The AMU performed a number of sensitivity tests in order to determine the best model configuration for operational use at each of the ranges to best predict winds, precipitation, and temperature (Watson 2013). This report details the continuation of that work and provides a recommended local data assimilation (DA) and numerical forecast model design optimized for the ER and WFF to support space launch activities.

## 2. DATA AND MODEL CONFIGURATION

The important aspects of this study were choice of DA software, the observational data ingest, period of record (POR), the DA/model configurations, and the DA/modeling system Perl scripts supplied by SPoRT.

### *2.1 Data Assimilation Software*

DA is an important component in producing quality numerical weather prediction forecasts. DA methods are used to create a best estimate of the state of the atmosphere at the forecast initial time using information from observations and a background model forecast. This is accomplished through the minimization of an objective function that measures the weighted distance of the analysis from the observations and the background model. The weights assigned to each term are based on the error characteristics of the observations and the background model (Kleist et al. 2009). This creates an initial state that more closely resembles the state of the atmosphere at the model initialization time.

The DA software chosen for this task was the Gridpoint Statistical Interpolation (GSI) system developed by the National Centers for Environmental Prediction (NCEP). The GSI system is a three-dimensional variational DA system that is a freely available, community system designed to be flexible, state-of-the-art, and can run efficiently on various parallel computing platforms. It can be applied to both regional and global applications.

### *2.2 Observational Data Ingest*

GSI can ingest large quantities of atmospheric observations and has developed capabilities for data thinning, quality controlling, and satellite radiance bias correction (Wang 2010). Table 1 lists some of the

[*] *Corresponding author address:* Leela R. Watson, ENSCO, Inc., 1980 North Atlantic Ave, Suite 830, Cocoa Beach, FL 32931; e-mail: watson.leela@ensco.com

conventional and satellite radiance/brightness temperature observations that GSI can assimilate.

Most of these observations are complex and many of them need to be reformatted into Binary Universal Form for the Representation of meteorological data (BUFR) format or quality controlled before being used by GSI. NCEP produces quality-controlled data in BUFR format, called PrepBUFR files that can be used directly in GSI.

### *2.3 Model Configuration and Test Cases*

The AMU determined the main model configuration from the first phase of the Range Modeling task. The ARW core was used with the Lin microphysical scheme and the YSU PBL scheme for both the ER and WFF. Although the AMU previous work found the optimal horizontal grid spacing for the ER was a 2-km outer and 0.67-km inner domain and a 4-km outer and 1.33-km inner domain for WFF, the AMU conducted additional testing on the optimal horizontal grid spacing once the DA was added. Specifically, different configurations were run to determine the impact on the forecasts of running the DA over differing grid resolutions. For the ER, the AMU ran three configurations:

- Single domain: 1-km domain in which the DA was run (referred to as '1 dom', Figure 1),
- Nested domain: 2-km outer and 0.67-km inner domain in which the DA was run on the outer 2-km domain (referred to as '2 doms', Figure 2),
- Triple nested domain: 9-km outer, 3-km middle, and 1-km inner domain on which the DA was run on the 9-km outer domain (referred to as '5 doms', Figure 3).

For WFF, the AMU ran two configurations:

- Nested domain: 4-km outer and 1.33-km inner domain in which the DA was run on the outer 4-km domain (referred to as '2 doms', Figure 4),
- Triple nested domain: 9-km outer, 3-km middle, and 1-km inner domain on which the DA was run on the 9-km outer domain (referred to as '5 doms', Figure 3).

All other parameters were the same for each model run.

Table 1. List of conventional and satellite observations that can be assimilated into GSI.

| **Conventional observations** | | |
|---|---|---|
| • Radiosondes<br>• Conventional aircraft reports<br>• MODIS IR and water vapor winds<br>• Surface land observations<br>• Doppler radial velocities<br>• SBUV ozone profiles, MLS (including NRT) ozone, and OMI total ozone<br>• Wind profilers: US, JMA<br>• Dropsondes<br>• GEOS hourly IR and coud top wind<br>• GPS Radio occultation refractivity and bending angle profiles | • Pibal winds<br>• ASDAR aircraft reports<br>• GMS, JMA, and METEOSAT cloud drift IR and visible winds<br>• SSM/I wind speeds<br>• VAD (NEXRAD) winds<br>• SST<br>• Doppler wind Lidar data<br>• Tail Doppler Radar radial velocity and super-observation<br>• METAR cloud observations<br>• SSM/I and TRMM TMI precipitation estimates | • Synthetic tropical cyclone winds<br>• MDCARS aircraft reports<br>• EUMETSAT and GOES water vapor cloud top winds<br>• QuikScat, ASCAT and OSCAT wind speed and direction<br>• GPS precipitable water estimates<br>• Tropical storm VITAL<br>• Radar radial wind and reflectivity Mosaic<br>• PM2.5<br>• Surface ship and buoy observation |
| **Satellite radiance/brightness temperature observations** | | |
| • SBUV: n17, n18, n19<br>• AIRS:aqua<br>• MHS: metop-a, metop-b, n18, n19<br>• AMSRE: aqua<br>• GOME: metop-a, metop-b,<br>• ATMS: NPP | • HIRS: metop-a, metop-b, n17, n19<br>• SSMI: f14, f15<br>• SNDR: g11, g12, g13<br>• OMI: aura<br>• SEVIRI: m08, m09, m10 | • GOES_IMG: g11, g12<br>• AMSU-A: metop-a, metop-b, n15, n18, n19, aqua<br>• AMSU-B: metop-b, n17<br>• SSMIS: f16<br>• IASI: metop-a, metop-b |

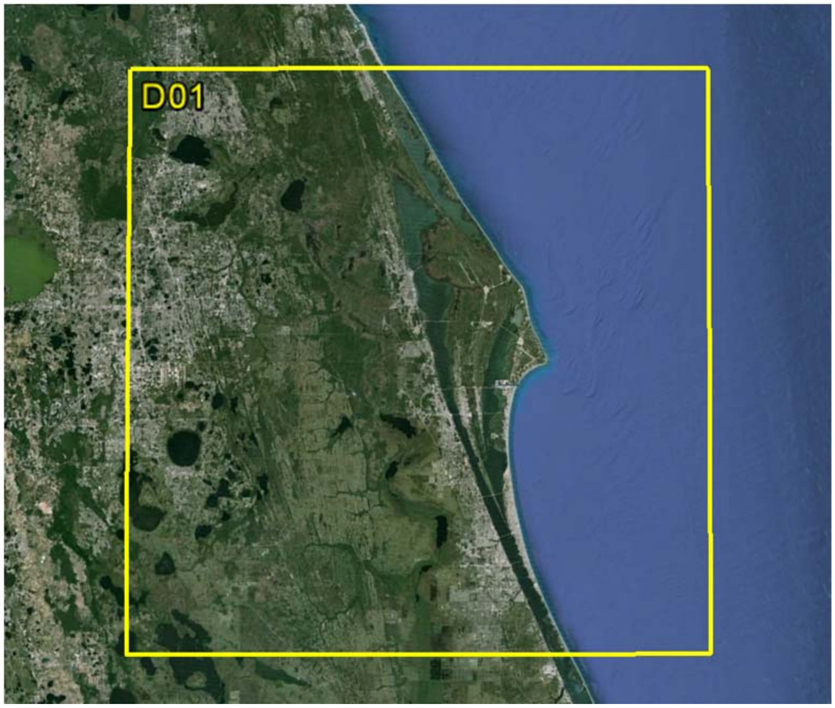


Figure 1. Map of the ER showing the single 1-km (D01) model domain boundary (1 dom).

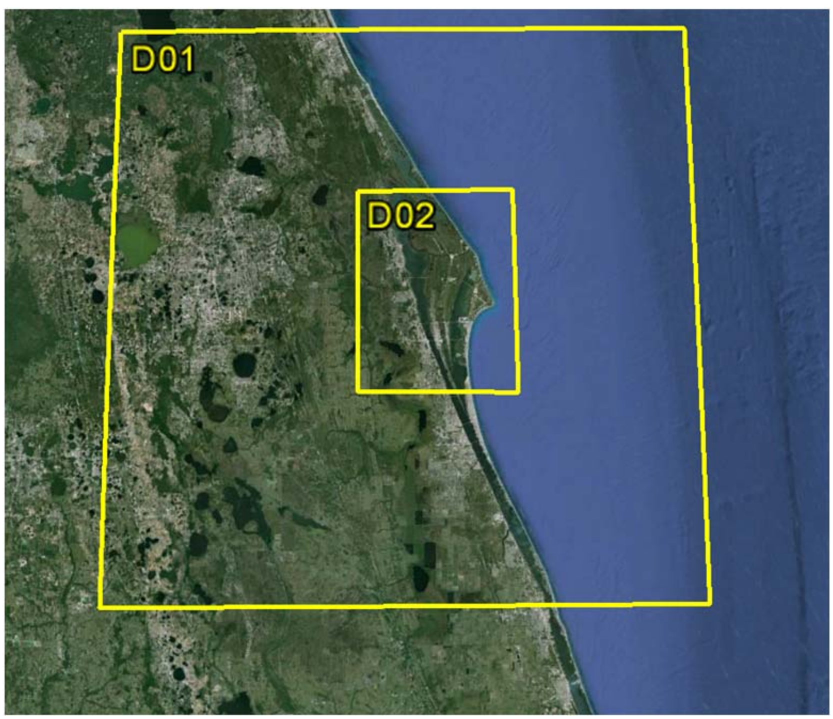


Figure 2. Map of the ER showing the nested 2-km outer (D01) and 0.67-km inner (D02) model domain boundaries (2 doms).

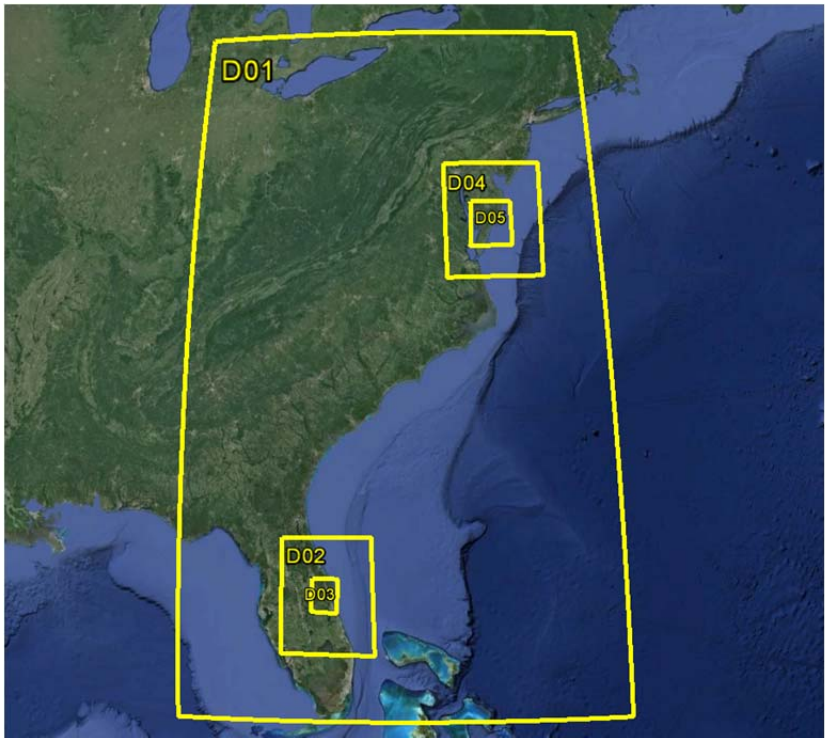


Figure 3. Map of the triple nest configuration showing the 9-km outer (D01), 3-km middle (D02 and D04), and 1-km inner (D03 and D05) model domain boundaries over the ER and WFF (5 doms).

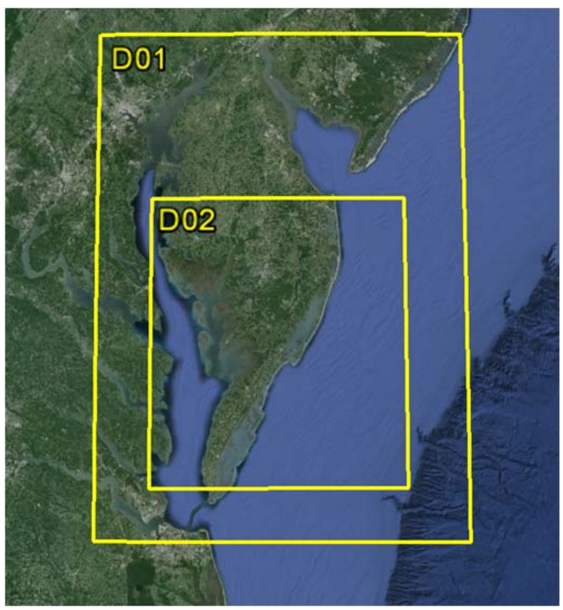


Figure 4. Map of WFF showing the nested 4-km outer (D01) and 1.33-km inner (D02) model domain boundaries (2 doms).

The AMU ran each DA/model simulation at the specified horizontal resolution with 35 irregularly spaced, vertical sigma levels up to 50 mb. Each run was initiated four times per day at 0000, 0600, 1200, and 1800 UTC and integrated 12 hours using the 13-km Rapid Refresh (RAP) model for boundary conditions and as the background model first-guess field, Land Information System (LIS) data from SPoRT for land surface data, and sea surface temperature (SST) data from both NCEP's Real-time Global SSTs and the SPoRT 2-km SST composites. Initial conditions were created using a cycled GSI/WRF approach that is described in Section 0. The POR for the test cases was from 1200 UTC 27 August 2013 to 0600 UTC 10 November 2013.

### *2.4 NASA SPoRT Perl Scripts*

SPoRT provided a set of Perl scripts that run both the GSI DA system and the WRF model in a compact system. The objective of the scripts is to provide an easy-to-use interface for users to be able to execute GSI and WRF. The SPoRT scripts are simply a wrapper to support running of the software systems, which must be downloaded and installed separately by the user.

The GSI/WRF scripts use a cycled GSI system similar to the operational North American Mesoscale (NAM) model. The scripts run a 12-hour pre-cycle in which data are assimilated from 12 hours prior up to the model initialization time. This is done due to the time latency of the satellite data. Satellite data are not available instantaneously as it takes time to receive and process. If the pre-cycling did not occur, there would be very little influence on model output from the satellite observations, which have been shown to have the largest positive impact on most forecast systems. Once the pre-cycling is complete, a 12-hour forecast is run.

A schematic of the GSI/WRF pre-cycling system is shown in Figure 5. Model initialization times are shown in green, pre-cycle times are shown in blue, and forecasts are shown in red. As stated above, the model is run four times per day. For a model initialization time of 0000 UTC (t00Z in Figure 5), the GSI/WRF scripts are started between 0000 and 0100 UTC. The scripts begin their pre-cycling 12 hours prior to initialization time, in this case at 1200 UTC of the previous day. Initial conditions for the WRF forecast are first created by processing the RAP data as the background model, the LIS land surface data, and NCEP and SPoRT SST data using the WRF preprocessing system. Once a background grid has been established, observational data are assimilated into the background grid using the GSI system. After the observations have been assimilated, a 3-hour WRF forecast is run (red arrow between tm12 and tm09 for t00Z). The pre-cycle begins again using data from nine hours prior to the initialization time (tm09, 1500 UTC of the previous day), however, the 3-hour WRF forecast is now used as the background model for the next forecast. This process continues every three hours until the initialization time is reached. At 0000 UTC after the background grid is created using the 3-hour WRF forecast and the observational data is assimilated, a 12-hour WRF forecast is run (red dashed line). The process repeats itself every six hours.

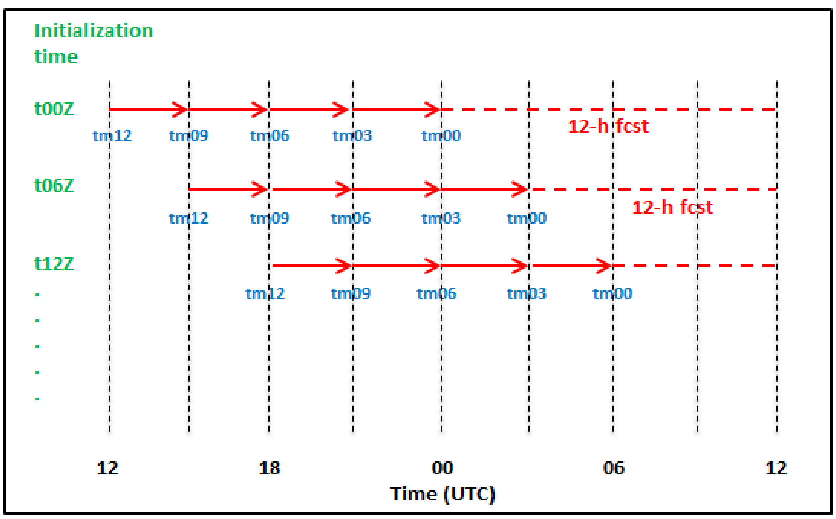


Figure 5. Schematic showing the 12-hour pre-cycling that occurs in the GSI/WRF system. Text in green is the model initialization time, solid red arrows are the pre-cycle forecast, and red dashed arrows are the full model forecast. This figure is a recreation of a NASA SPoRT produced schematic.

## 3. MODEL FORECAST VALIDATION

The AMU validated the GSI/WRF model forecasts using statistics that compared locally available surface observations to the forecast data. Precipitation forecasts were compared to nationally available rainfall data using a technique developed at NCAR.

### *3.1 Observational Data*

In order to verify the GSI/WRF model performance, surface weather observations of temperature, dewpoint, wind speed and direction, and atmospheric pressure were required. NCEP's Meteorological Assimilation Data Ingest System (MADIS) and Stage IV precipitation data were used for the observational datasets.

For this task, the AMU downloaded METAR and mesonet data to validate the GSI/WRF forecasts. To verify precipitation, the AMU compared hourly forecast rainfall accumulation to the NCEP Stage-IV analysis (http://www.emc.ncep.noaa.gov/mmb/ylin/pcpanl/stage4/). This analysis combines radar data and rain gauge reports to produce hourly rainfall accumulation on a 4-km grid. It is a manually quality-controlled continental U.S. mosaic from the regional 1-hour precipitation analyses produced by 12 National Weather Service River Forecast Centers (Lin and Mitchell 2005).

### *3.2 MET Software*

For the objective analysis, the AMU compared observed wind speed, temperature, dewpoint temperature, mean sea-level pressure, and accumulated precipitation observations to the forecast variables using the latest version of the Model Evaluation Tools (MET) software. This software was developed by the NCAR Developmental Testbed Center. It is a state-of-the-art suite of verification tools that uses output from the WRF model to compute standard verification scores comparing gridded model data to point or gridded observations, and uses spatial verification methods comparing gridded model data to gridded observations using object-based decomposition procedures. For this task, two MET tools were chosen to validate the GSI/WRF forecasts: the Point-Stat tool and the MODE tool.

The MET Point-Stat tool was used to verify the surface forecasts. This tool provides verification statistics for forecasts at observation points, in this case, at the METAR and mesonet point observations. The Point-Stat tool matches gridded forecasts to point observation locations using a user-specified interpolation approach and computes the verification statistics.

Many output statistics are available within the Point-Stat tool. This study looked at three of those statistics for wind speed, temperature (T), dewpoint temperature ($T_d$), and mean sea-level pressure (MSLP): the ME, the RMSE, and the PCC; and two statistics for wind direction: the ME and the RMSE. The statistics compared all mesonet and METAR observations available to the corresponding locations in the model forecast output at a 1-hour interval.

The mean error, ME, is a measure of the overall bias of the model parameter being compared. A perfect forecast has ME = 0. It is defined as:

$$ME = \frac{1}{n}\sum_{i=1}^{n}\left(f_i - o_i\right)$$

where:

$n$ = number of forecast and observation pairs over the forecast period,

$f_i$ = WRF forecast of T, $T_d$, MSLP, wind speed, or wind direction, and

$o_i$ = observed T, $T_d$, MSLP, wind speed, or wind direction.

The model RMSE was calculated to measure the magnitude of the error. It is useful in determining whether the forecasts produced large errors, as it gives relatively high weight to large errors. It is calculated using the following equations:

$$MSE = \frac{1}{n}\sum_{i=1}^{n}(f_i - o_i)^2$$

$$RMSE = \sqrt{MSE}$$

where $n$, $f_i$, and $o_i$ are defined as above.

The PCC, $r$, measures the strength of the linear association between the forecast and observed parameters. It is defined as:

$$r = \frac{\sum_{i=1}^{n}\left(f_i - \overline{f}\right)\left(o_i - \overline{o}\right)}{\sqrt{\sum_{i=1}^{n}\left(f_i - \overline{f}\right)^2 \sum_{i=1}^{n}\left(o_i - \overline{o}\right)^2}}$$

where $n$, $f_i$, and $o_i$ are defined as above and:

$\overline{f}$ = average forecast over time and space of T, $T_d$, MSLP, wind speed, or wind direction, and

$\overline{o}$ = average observed over time and space of T, $T_d$, MSLP, wind speed, or wind direction.

The PCC can range between -1 and 1 where 1 indicates a perfect correlation, -1 indicates a perfect negative correlation, and 0 indicates no correlation between the forecast and observations. For example, the PCC for wind speed measures whether large values of forecast wind speed tend to be associated with large values of observed wind speed (positive correlation), whether small values of forecast wind speed tend to be associated with large values of observed wind speed or vice versa (negative correlation), or whether values of both variables are unrelated (correlation near 0).

To verify precipitation, the AMU compared the forecast hourly rainfall accumulation to the observed rainfall over the same time period. MODE was used to determine the skill of each model configuration. MODE is an object-based verification system that compares gridded observations to gridded forecasts. It resolves and compares objects, such as areas of accumulated rainfall, in both the forecast and observed fields. The objects are described geometrically and then the attributes of the objects can be compared (Davis et al. 2006). MODE outputs statistics that describe the correlation between the objects and allows the user to identify forecast strengths or weaknesses. Details about how objects are identified and characterized can be found in Davis et al. (2006). For this report, the objects of interest are areas of accumulated rainfall. Therefore, references to objects are references to areas of resolved accumulated rainfall throughout the forecast period.

Once the objects have been identified, their various properties are evaluated and compared. The object attributes examined by the AMU in this task included the centroid distance, area ratio, and total interest value. The centroid distance is the vector difference between the centroids of the forecast and observed objects. It describes the location bias in the forecasts. The smaller the distance between the centroids, the better the forecast. The area ratio compares the area, or number of grid squares, the forecast object occupies compared to the observed object. An area ratio of 1 is considered a perfect correlation. Interest value is defined as the differences in particular attributes between the forecast and observed objects. Interest values of 0 indicate no interest, or a poor forecast, while a value of 1 indicates high interest, or a good forecast. The total interest value is a weighted sum of specific interest values and is used as an overall indicator of the quality of the precipitation forecast. Total interest value is large when forecast and observed objects are well correlated (are roughly the same size and are close to each other) and is small when they are not well correlated.

## 4. ER RESULTS

The AMU validated model performance for the ER using forecasts from the grids described in section 0, where 2 doms references the nested 2-km outer and 0.67-km inner domain (Figure 2), 1 dom references the single 1-km domain (Figure 1), and 5 doms references the triple nested 9-km outer, 3-km middle, and 1-km inner domain over the ER (Figure 3).

### *4.1 Surface Forecasts*

The AMU validated the GSI/WRF forecasts with the local METAR and mesonet data. Figure shows the ME for wind speed, wind direction, temperature, dewpoint temperature, and MSLP from the three GSI/WRF configurations averaged over each hour of each 12-hour forecast for the entire POR at the ER.

Overall, the ME results indicate that the triple-nest configuration performed the best of the three configurations, followed by the nested domain, and then the single domain. The triple-nest configuration had the lowest ME for wind speed, wind direction, dewpoint temperature, and MSLP while the nested domain had the lowest ME for temperature. The single domain had the highest ME for wind speed, temperature, and dewpoint temperature.

The average hourly ME results for wind speed indicated that all three domain configurations over-predicted the wind speed throughout the forecasts. The ME for wind speed for the single domain was approximately 2 m/s higher than for either nested domain during the entire forecast period with an average hourly ME of approximately 5 m/s. All three domains followed the same trend of slightly increasing ME throughout the forecasts for wind direction. The single domain had a consistent warm bias throughout the forecasts as indicated by the average hourly ME for temperature with a maximum ME of approximately 0.7 K. Both nested domains exhibited a cool bias throughout the forecasts, except for the 0-hour forecast. All domain configurations exhibited a cool dewpoint temperature bias, with the single domain showing the largest cool bias in the 2 to 2.3 K range. Results from the average hourly ME for MSLP show that all three configurations followed the same trend of an initial negative, or low pressure, bias followed by a slight positive, or high pressure, bias.

As with ME, the RMSE results indicate that the triple-nest configuration performed the best of the three configurations, followed by the nested domain, and then the single domain. The triple-nest configuration had the lowest RMSE for wind speed, wind direction, and dewpoint temperature while the nested domain had the lowest RMSE for temperature and MSLP. The single domain had the highest RMSE for all variables except wind direction.

The PCC can indicate whether the model configurations captured the overall trend of the observed variables. Using wind speed as an example, it answers the question of whether the model winds fluctuated positively and negatively with the same magnitude as the observed winds. The closer the PCC is to 1, the better the model was able to capture these trends. When comparing these particular forecast vs. observed variables, only positive coefficients indicate any value in the model forecasts.

The results from the PCC (Figure ) calculation indicate that the triple-nested configuration again performed the best of the three configurations followed by the single domain and then the nested domain. The triple-nest configuration had the highest PCC for wind speed, temperature, and MSLP while the single domain had the highest PCC for dewpoint temperature.

All results show a positive correlation, except for the nested domain during forecast hours 8-9 for MSLP indicating that the fluctuations in each of the variables was captured by the model. However, overall the values for PCC were low. This may be due to the difficulty in capturing mesoscale phenomena in the summertime over the ER.

### *4.2 Precipitation Forecasts*

The AMU compared precipitation forecasts from all three model configurations to determine performance differences. One-hour forecast accumulated rainfall for each hour of each of the 12-hour forecasts was compared to the one-hour accumulation of observed rain using the NCEP Stage-IV analysis data for each day during the POR. The POR summary statistics for each hour of the forecast of centroid distance, area ratio, and total interest value from the MODE software are shown in Figure . The centroid distance (km) results indicate that the nested domain precipitation matched the location of the observed precipitation most closely throughout the forecasts, followed by the triple-nest configuration and then the single domain. The area ratio for the nested domain indicates that the forecast most closely matched the areal coverage of observed precipitation, with the triple-nest and single domain performing slightly worse and similarly, respectively. Interest value functions near 0.9 for the nested domain indicates that overall the forecast correlated the best with the observed precipitation, followed by the triple-nest configuration and then single domain. Overall, the nested domain outperformed both triple-nest and single domain configurations.

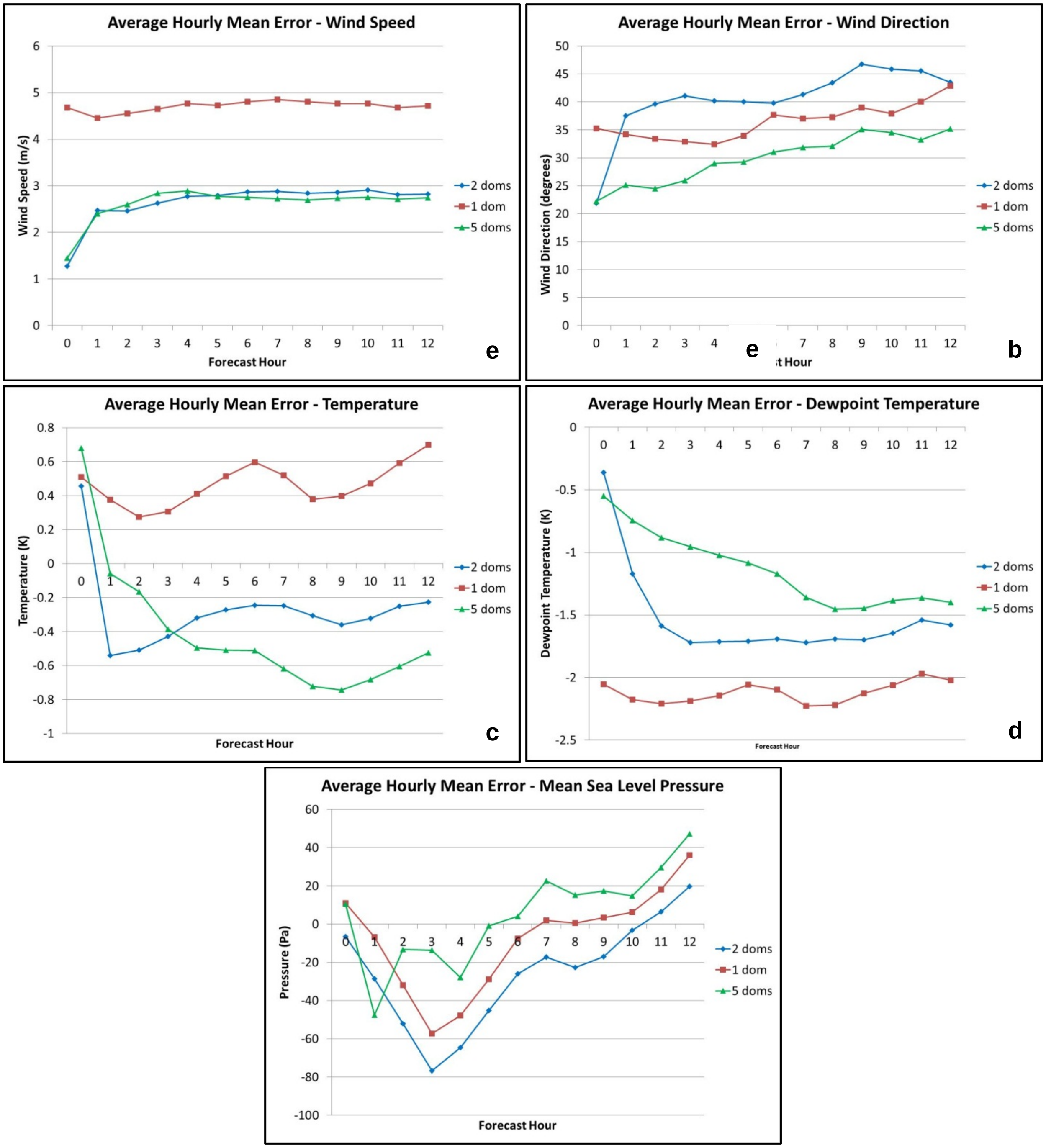


Figure 6. Chart of the average hourly ME for the 12-hour forecast over the entire POR for a) wind speed, b) wind direction, c) temperature, d) dewpoint temperature, and e) MSLP from the three GSI/WRF configurations at the ER

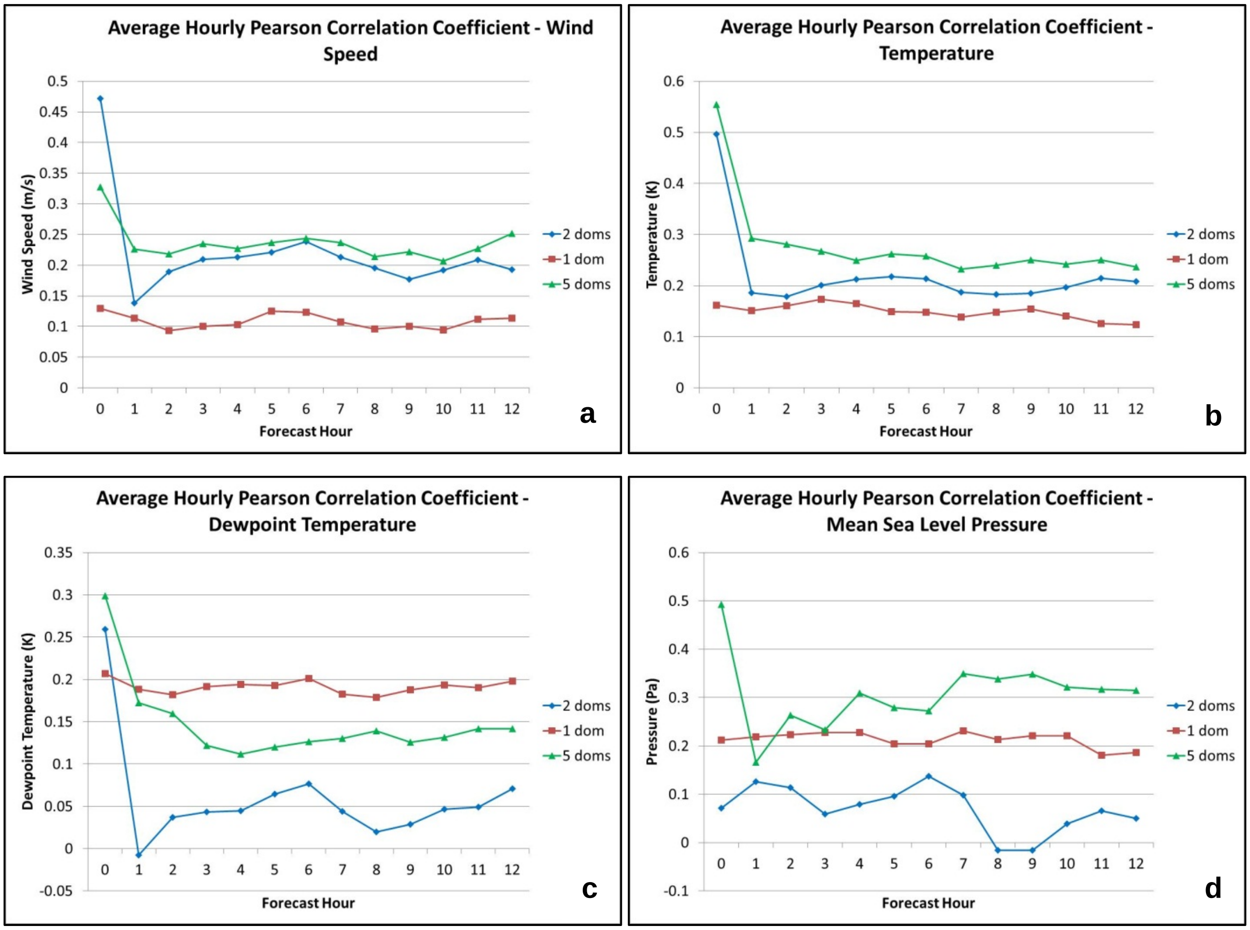


Figure 7. Chart of the average hourly PCC for the 12-hour forecast over the entire POR for a) wind speed, b) temperature, c) dewpoint temperature, and d) MSLP from the three GSI/WRF configurations at the ER.

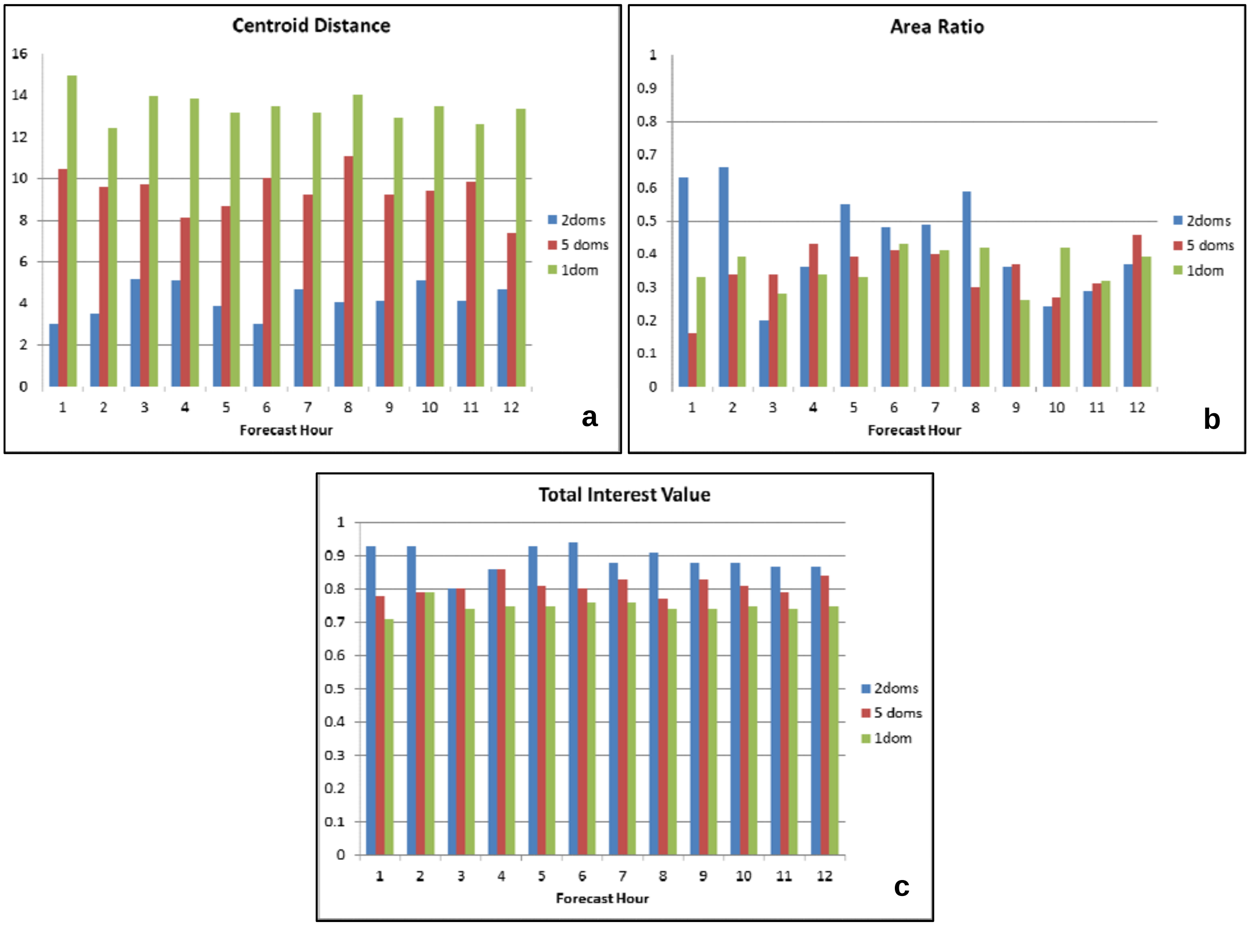


Figure 8. Chart of the average hourly a) centroid distance (km), b) area ratio, and c) total interest value from the three GSI/WRF configurations for each hour of the 12-hour forecast over the entire POR at the ER.

## 5. WFF RESULTS

The AMU validated model performance for WFF using forecasts from the grids described in section 0, where 2 doms references the nested 4-km outer and 1.33-km inner domain (Figure 4) and 5 doms references the triple-nested 9-km outer, 3-km middle, and 1-km inner domain over WFF (Figure 3).

### *5.1 Surface Forecasts*

The AMU validated the GSI/WRF forecasts with the local METAR and mesonet data. Figure  shows the ME for wind speed, wind direction, temperature, dewpoint temperature, and MSLP from the two GSI/WRF configurations averaged over each hour of each 12-hour forecast for the entire POR at WFF.

Overall, the ME results indicate that the triple-nest configuration performed better than the nested domain. The triple-nest configuration had the highest ME for wind speed, wind direction, temperature, and MSLP while the nested domain had the highest ME for dewpoint temperature.

Both model configurations over-predicted the wind speed throughout the forecast with a large increase in ME after the first forecast hour. However, the error for the triple-nest configuration was nearly 1.5 m/s less than that for the nested domain throughout the forecast. The same large increase after the first forecast hour in ME for wind direction was present in the nested domain with slightly decreasing values of ME after forecast hour 3, while the triple-nest configuration showed gradual increasing ME error values throughout the forecast period. The triple-nest configuration had lower ME values than the nested domain with differences in ME of approximately 15 to 30 degrees. ME values for temperature were nearly the same for both configurations during the first five forecast hours, after which the triple-nest configuration outperformed the nested domain with ME values of nearly 0. The triple-nest configuration consistently forecasted dewpoint temperature values that were too cool, while the nested domain was too cool during the first 5 hours and then too warm after that. Both configurations followed the same ME trend for MSLP with pressures that were initially too low and then too high in the latter part of the forecasts.

Similar to the ME, the RMSE results indicate that the triple-nest configuration performed the best for all variables. The RMSE wind speed and direction charts are nearly identical to the ME error charts indicating that there were not any large outliers for forecasted wind speed or direction. The triple-nest configuration RMSE for temperature and dewpoint temperature was roughly 1.25 K lower than that for the nested domain throughout the forecasts. Except for forecast hours 2 and 3, the triple-nest configuration outperformed the nested domain for MSLP with differences of approximately 60 Pa lower in the latter half of the forecasts.

The results from the PCC calculation (Figure 10) indicate that the triple-nest configuration again outperformed the nested domain for wind speed, temperature, dewpoint temperature, and MSLP. The PCC for the triple-nest configuration for wind speed and temperature was approximately 0.05 to 0.1 higher than the nested domain throughout the forecast. The PCC for dewpoint temperature was 0.2 to 0.3 higher for the triple-nest configuration and was up to 0.1 higher through forecast hours 4 to 11 than the nested domain for MSLP. It is interesting to note that the highest PCC values for WFF were nearly double that of the ER. During the summer and fall, different systems drive the local weather at each range. There are more synoptic systems that influence the weather over the WFF during summer and fall while in the summer, the weather over the ER is locally driven by mesoscale phenomena. In general, models will perform better when the local weather is driven by larger-scale synoptic systems. Therefore, it is expected that the GSI/WRF system performed better for WFF than for the ER during the POR.

### *5.2 Precipitation Forecasts*

The AMU compared precipitation forecasts from both model configurations to determine performance differences. One-hour forecast accumulated rainfall for each hour of each of the 12-hour forecasts was compared to the one-hour accumulation of observed rain using the NCEP Stage-IV analysis data for each day during the POR. The POR summary statistics for each hour of the forecast of centroid distance, area ratio, and interest function from the MODE software are shown in Figure 11Figure . The centroid distance (km) results indicate that forecasts from both configurations were very similar in their ability to match the location of the observed precipitation throughout the forecasts. However, the triple-nest configuration did slightly better in predicting the precipitation location. The area ratio results indicate that accumulated precipitation for the triple-nest configuration matched the areal coverage of observed precipitation more closely, although the results were comparable. Total interest values were very similar for both configurations with values near 0.8. Overall, the triple nest configuration very slightly outperformed the nested domain.

## 6. CONCLUSIONS

This report summarizes the findings from the AMU task to determine a recommended local DA and numerical forecast model design optimized for the ER and WFF to support space launch activities and for local weather forecasting challenges at each range. The AMU ran the GSI/WRF model system over part of the summer and fall seasons for each range while varying grid resolutions on which the DA was run and varying the nesting configurations to determine the impact on model skill. In general for both the ER and WFF, the triple-nest configuration outperformed the other configurations. However, although the results for the ER indicate that the triple-nest configuration performed best for most variables as evidenced by the ME, RMSE, and PCC, the nested configuration did the best in predicting precipitation for the ER. Summertime convection over the ER is an important meteorological variable to predict and, for this reason, it is the AMU’s recommendation to use either the nested or triple-nest configuration as the optimal model configuration for the ER. The triple-nest configuration performed the best for nearly all variables at WFF. Wind, temperature, and convective activity forecasts during the fall and spring seasons pose the most difficulties for forecasters at WFF. Therefore, it is the AMU’s opinion that the triple-nested domain is the optimal model configuration for WFF.

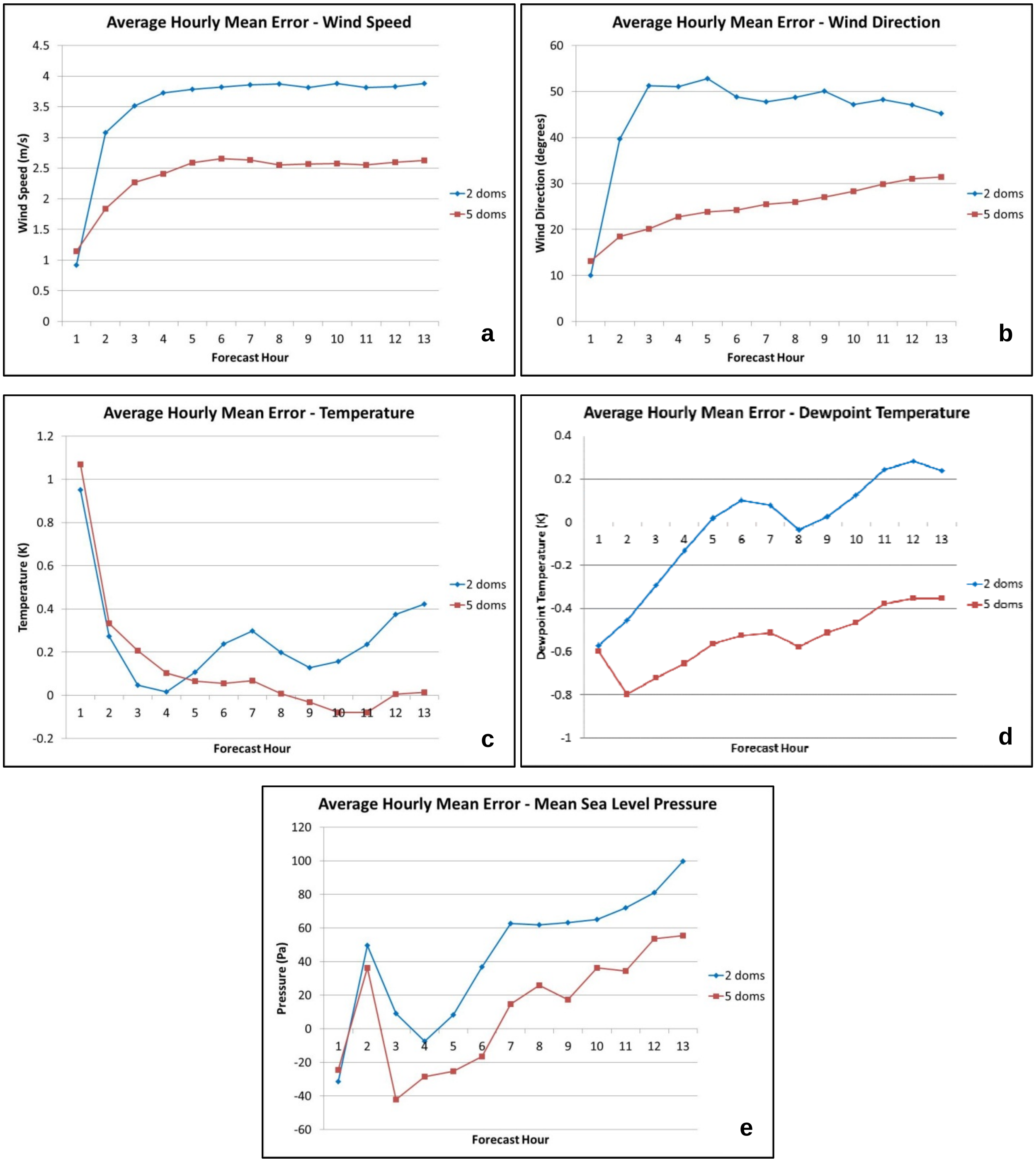


Figure 9. Chart of the average hourly ME for the 12-hour forecast over the entire POR for a) wind speed, b) wind direction, c) temperature, d) dewpoint temperature, and e) MSLP from the two GSI/WRF configurations at WFF.

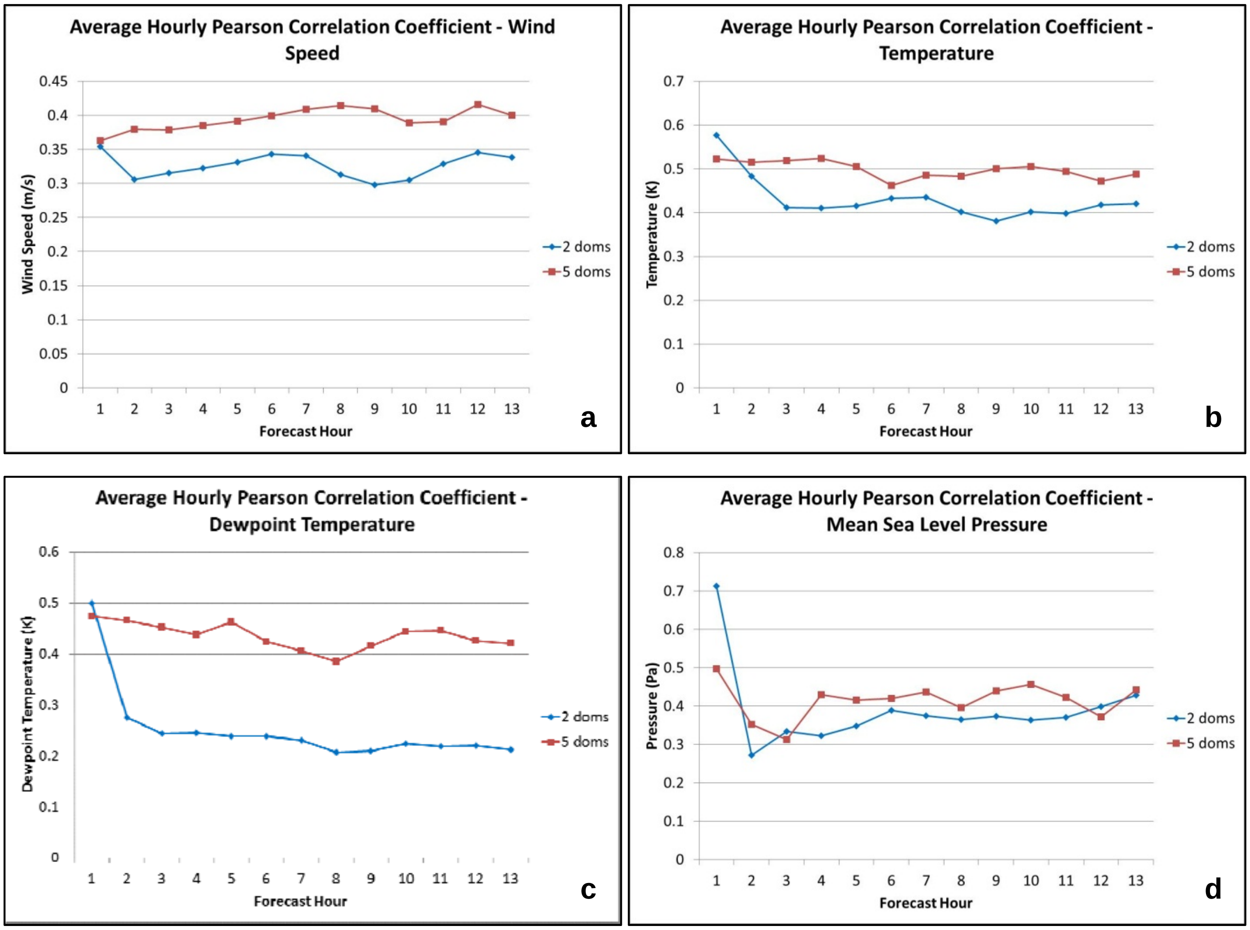


Figure 10. Chart of the average hourly PCC for the 12-hour forecast over the entire POR for a) wind speed, b) temperature, c) dewpoint temperature, and d) MSLP from the two GSI/WRF configurations at WFF.

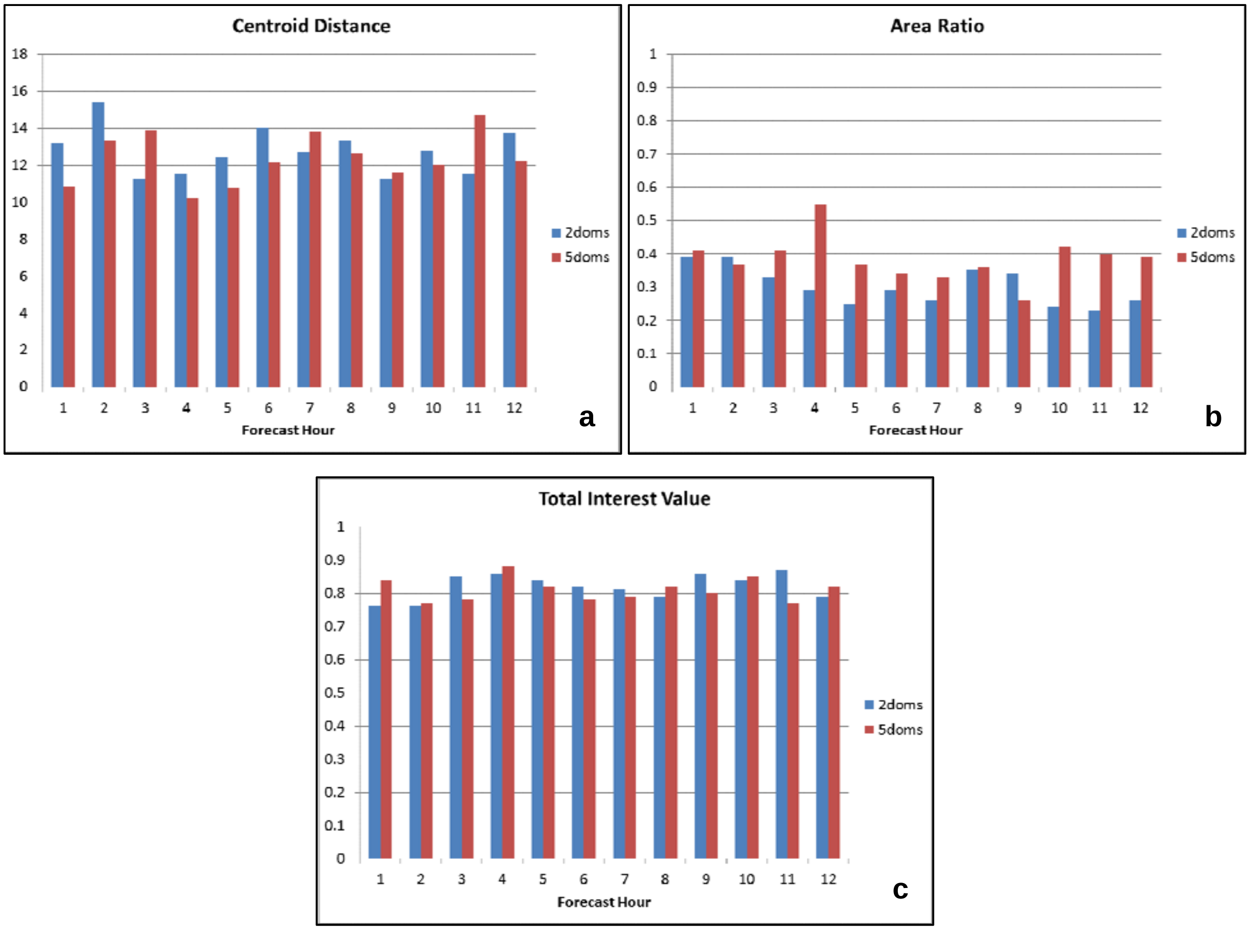


Figure 11. Chart of the average hourly a) centroid distance (km), b) area ratio, and c) total interest value from the two GSI/WRF configurations for each hour of the 12-hour forecast over the entire POR at WFF.

## 7. REFERENCES

Davis, C., B. Brown, and R. Bullock, 2006: Object-based verification of precipitation forecasts. Part I: Methods and application to mesoscale rain areas. *Mon. Wea. Rev.*, **134,** 1772–1784.

Kleist, D. T., D. F. Parrish, J. C. Derber, R. Treadon, W. Wu, S. Lord, 2009: Introduction of the GSI into the NCEP Global Data Assimilation System. *Wea. Forecasting*, 24, 1691–1705.

Lin, Y. and K. E. Mitchell, 2005: The NCEP Stage II/IV hourly precipitation analyses: development and applications. Preprints, *19th Conf. on Hydrology*, San Diego, CA, Amer. Meteor. Soc., P1.2. [Available online at ams.confex.com/ams/Annual2005/techprogram/paper_83847.htm.]

Wang, Xuguang, 2010: Incorporating ensemble covariance in the Gridpoint Statistical Interpolation variational minimization: A mathematical framework. *Mon. Wea. Rev*., **138**, 2990–2995.

Watson, L., 2013: Range-specific High-resolution Mesoscale Model Setup. NASA Contractor Report CR-2013-217911, Kennedy Space Center, FL, 41 pp. [Available from ENSCO, Inc., 1980 N. Atlantic Ave., Suite 830, Cocoa Beach, FL, 32931 and online at http://science.ksc.nasa.gov/amu/final-reports/range-specific-hi-res-model-setup.pdf.]